Calibration of force sensing resistors (fsr) for static and dynamic applications

J.A. Flórez[1], A.Velásquez[2]
Product Design Engineering Department
EAFIT University
Medellin, Colombia
[1]jfloreze@eafit.edu.co, [2]avelasq9@eafit.edu.co

***Abstract*— This article shows a procedure to calibrate Force Sensing Resistors (FSR), whose manufacturers rarely offer calibration details. Literature and experience show that, due to the nature of FSR construction, its time dependency makes it hard to calibrate at first glance by simple measurements. The methodology employed is based upon the comparison of the measured data obtained from a FSR with the one obtained from a calibrated load cell. The force loading and unloading processes are performed automatically with a mechatronic device which allows having time invariant and variant force profiles. Special analysis is taken over creep and hysteresis compensation along with its relation with static and dynamic applications with the help of existing literature. At the end a time dependant function is obtained that relates the force applied on the sensor, and the signal obtained from it, allowing for the use on applications to measure force and pressure in ranges from 0 to 20N and 0 to 100mmHg respectively.**

Keywords-FSR;calibration; creep; hysteresis

I. INTRODUCTION

The Force Sensing Resistors (FSR) are devices that allow measuring static and/or dynamic forces applied on a surface where it is placed, through the variation of its electric resistance. There are several manufacturers of such sensors in the market, with very similar architecture and working principles, being their principal advantages, low cost per-unit, human touch applications calibration (forces below 10Kg), little space required for installation (thicknesses under 1.25mm) and high variety in shapes and sizes [1] and [2].

Despite of these advantages, its reliable use on products depends on a prior proper calibration method and a digital handling to deal with the force values.

By theory it is considered that when a force is applied the change of the sensor's electric resistance is approximately linear in a logarithmic plot [1] although things get different when time plays around. Hence the objective of a proper calibration besides relating the electric resistance value of the sensor with the applied force is to compensate creep and hysteresis when a time constant and variable force respectively is applied.

II. METHODOLOGY

The sensor to be calibrated is an Interlink Electronics 402 FSR, which has a sensing area of 12.7mm diameter. The sensor was connected to an electronic circuit, recommended by the manufacturer for high resolution and low value range measurements on dynamic applications. The circuit consists on a Voltage-to-Current converter (Fig. 1(a)), with the FSR resistance value as an input, and an inverse voltage variation (from 0V to V_{REF}) as an output *(V)*. The value of the RM resistor is chosen to maximize the level of sensitivity in the work range, and to limit the current through the sensor [1].

In addition, following the technique of [3] cited in [4], a rigid coating was added to the sensor, in this case a 12.7mm diameter and 3.3mm thick dome made of fiberglass resin using a nylon mould. The dome is attached to the sensing area of the sensor using thin double-sided tape (Fig. 1(b)). This helps to evenly distribute the force applied to the sensor over its entire surface, allowing to measure pressure (besides force) and avoiding the sensor to become saturated from punctual applied loads.

Labview software was used for data acquisition and a PCI 6013 data acquisition card (NI-DAQ), both from National Instruments [5]. A perspective view of the assembly of the calibration system is shown in Fig. 2, which was developed to apply a controlled force to a FSR placed between a calibrated load cell and a metal header. Thus both signals from the load cell and FSR can be simultaneously acquired and used to perform a mathematical regression process.

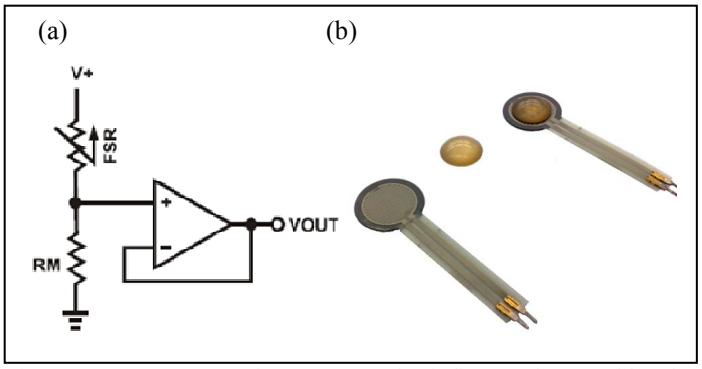

Figure 1. (a) Current-to-Voltage converter circuit diagram. (b) FSR with and without a resin dome.

Thanks to EAFIT University, as single sponsor of this project.

978-1-4244-6742-6/10/$26.00 ©2010 IEEE

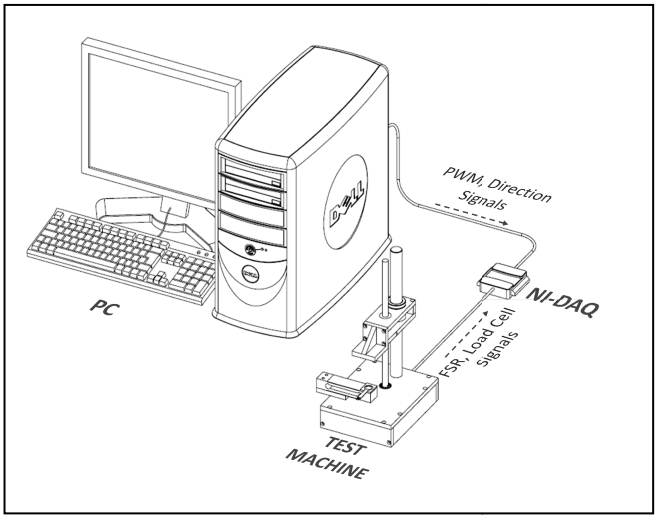

Figure 2. Components of the calibration and data acquisition system.

The compression force is generated through a nut-screw mechanism driven by a geared electric dc motor, which moves up and down, loading and unloading the FSR-load cell ensemble. The voltage sent to the motor is then controlled from the PC by a feedback of the measured force, where PWM and direction signals are generated through the NI-DAQ.

III. PROCEDURE

A. Static Test

At the first stage of the process, calibrated weights were statically placed over the sensor in order to obtain a relation between the applied force and the output voltage of the circuit. These weights and its increment between each reading were chosen according to the value of *RM* in such a way to remain between the limits of the sensor.

An algorithm was implemented in Labview to acquire the *(V)* signal from the circuit and to plot a voltage vs. time graph, while storing the data in a text file for post-processing. The curves formed with this data are discrete and discontinuous in time(Fig. 3(a)). An arithmetic mean value of voltage is calculated for each weight in order to obtain a Force vs. Voltage plot and its respective regression. The dispersion graph approximates to that of a logarithmic function (Fig. 3(b)).

Nevertheless these tests showed the existence of an undesired behavior of the sensor, creep as seen in Fig. 4, as a consequence of the FSR's electric resistance decrease in time. In order to overcome the creep behavior, the Labview algorithm was modified by obtaining the derivative in time of the acquired voltage signal. Hence the derivative value becomes a criterion at determining if an increase of the signal corresponds whether to an increase of the applied load, or creep behavior under static load conditions.

A range of allowable values for the derivative of the voltage must be defined when the applied load changes, in order to make this criterion useful. Thus, by using an automatic system, a 0.2Kg weight was placed and removed from the sensor with variable velocity. The velocity range was kept between 5mm/s and 30mm/s.

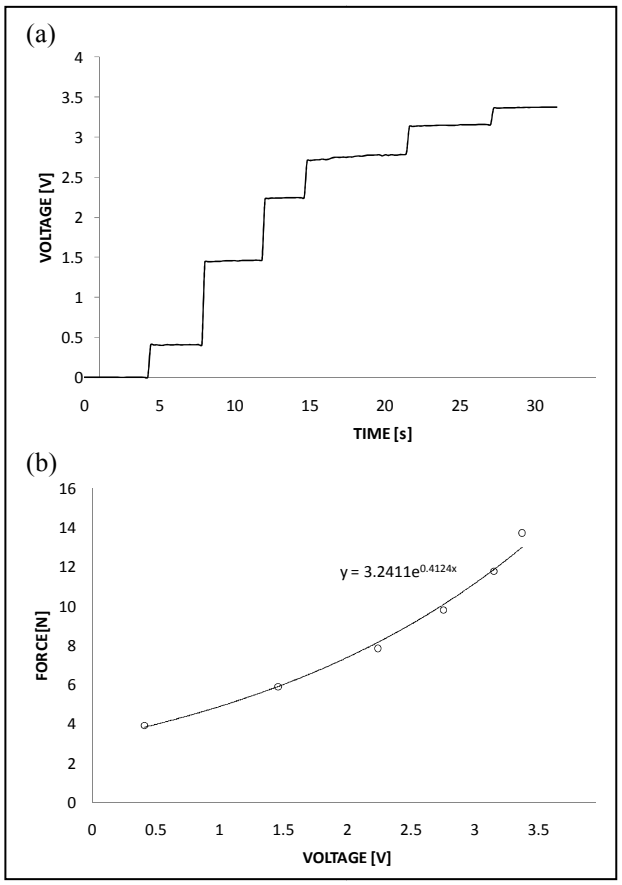

Figure 3. (a) Constant weight test. (b) Force Vs Voltage obtained with the arithmetic mean of the previous data.

As shown in Fig. 5(b) the derivative value increases when the load and unload velocity is increased; with its smallest registered value around 3.6V/s. Furthermore the typical values of the derivate, when the sensor is statically loaded, are below 0.2V/s. Therefore it can be determined that derivative values below 0.2V/s correspond to creep signals which should not be taken, instead keep the previous voltage value to determine the applied force.

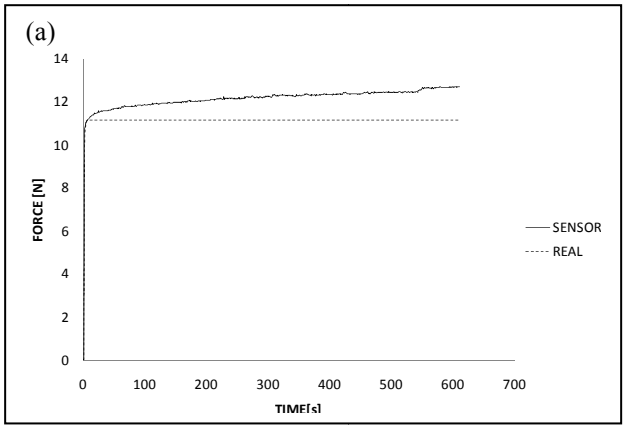

Figure 4. Creep evidence.

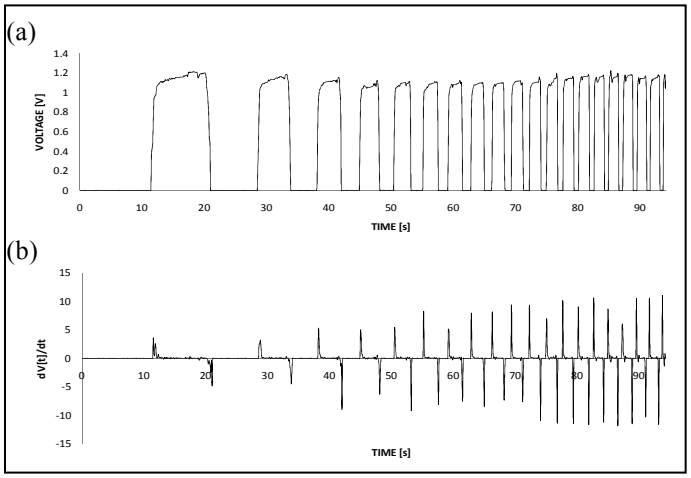

Figure 5. (a)Voltage Vs Time plot. (b)Values of the voltage derivative with variation of the load and unload velocity.

B. Dynamic Test

A dynamic test was performed by using the assembly shown in Fig. 2 which consisted on loading and unloading the sensor. In this case a second undesired behavior, although characteristic of the majority of the existent sensors, appeared. As seen in Fig. 6 during the loading stage the sensor follows the upper side of the curve, while during the unloading stage the measured voltage describes the lower side of the curve.

This behavior is one of the reasons why a hysteresis compensation strategy is discussed in [4], in which the force calculation depends not only on (*V*), but also on a moving integral (*I*), which is calculated by multiplying the measured voltage values obtained in the last 0.5s by a linear increasing factor and then summed. The values acquired before 0.5*s* are multiplied by zero. A 4th degree polynomial function is then obtained from a multiple regression as shown in (1).

$$F(V,I)=a_0+a_1V+a_2V^2+a_3V^3+a_4V^4+a_5I+a_6I^2+a_7I^3+a_8I^4 \quad (1)$$

Although this method's efficacy is proven in [4], other ways for calculating the moving integral were explored by varying two factors. Firstly, the amount of time of previous data to include was increased from 0.5s to 1s.

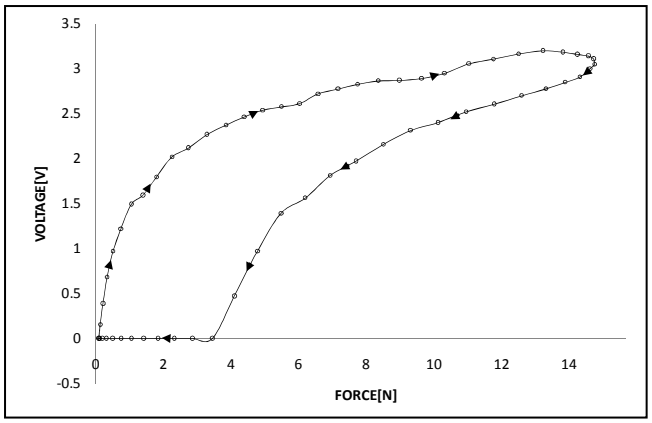

Figure 6. Hysteresis evidence.

Secondly the way of calculating the factors to be multiplied by the voltage data was changed from linear to logarithmic and exponential increasing. For each of these cases, standard error was calculated, and Real Force vs. Calculated Force graph was built to determine which of the cases brings the best result at hysteresis compensation. Moreover, a time independent regression was made, having the force only as a function of (*V*) in order to make a performance comparison.

IV. RESULTS

A. Creep compensation

A statically placed weight test was performed to implement the derivative criteria for creep correction, with a 0.2V/s as the minimum value to recognize that a (V) change was in fact due to a change in the sensor's load. The result obtained with this procedure, is shown in Fig. 7.

The algorithm modification consisted just on adding an if/else statement which ignores derivative values below 0.2V/s.

Such creep behavior can be analogously compared with a sponge, which when it is firstly squezeed reduces its thickness a certain amount, but after a while it would slowly continue reducing its thickness until reaching a certain limited value.

B. Hysteresis compensation

Regarding the hysteresis compensation, and performing a multiple regression with a web-based software [6] a set of results was achieved from the data collected by changing the way the variable *(I)* is calculated.

With comparative purposes, a single variable 4th degree polynomial regression was made, making (*F*) only voltage dependant, with the form of (2).

$$F(V)=b_0+b_1V+b_2V^2+b_3V^3+b_4V^4 \quad (2)$$

The graphical and numeric standard error is shown in Fig. 8(a) while hysteresis performance is shown in Fig. 8(b).

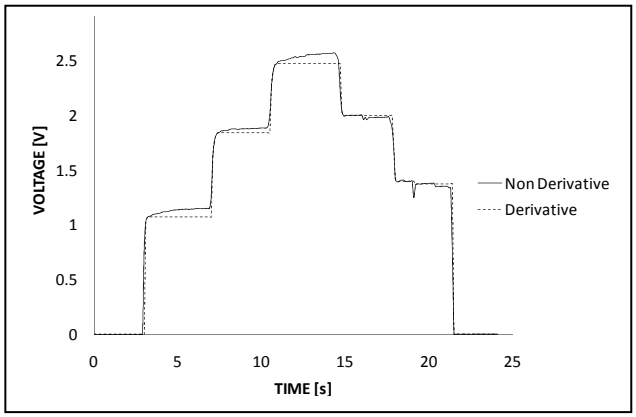

Figure 7. Result obtained when the derivate criteria was implemented to eliminate creep.

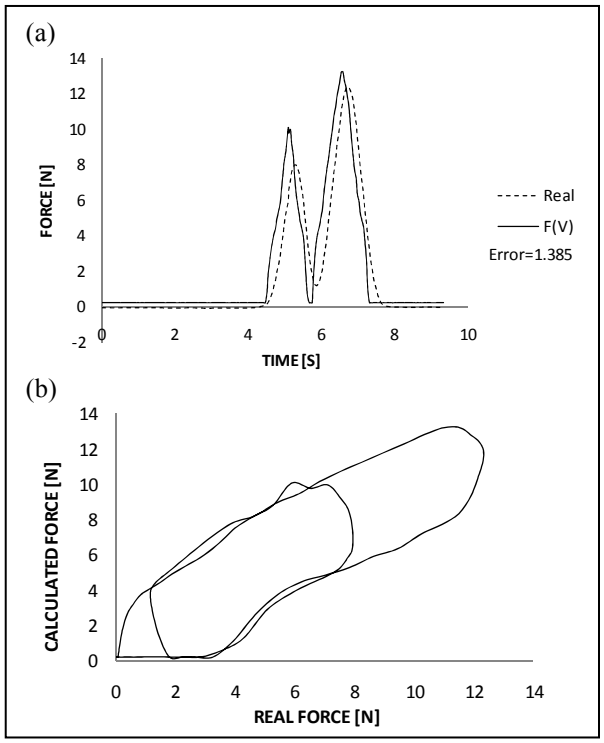

Figure 8. (a) Single variable regression graphical result, standard error. (b) Hysteresis performance under voltage dependence.

Table 1 shows the numeric results of the multiple 4th degree polynomial regression, while Fig. 9, Fig. 10 and Fig. 11 show the graphic comparison of the Real against Calculated force in time.

The reduction in the standard error of the regressions made with the moving integral factor varies between 15% and 73% when compared with the one that lacks of it. The smallest error belongs to the calculation made with linear increasing form and using the values of 0.5s which are the parameters used in [4].

It is important to point out that the calculated standard errors are comparable with each other because they are obtained from the same time and force data, indicating which regression achieves the best adjustment to the same curve

TABLE I. STANDARD ERROR OF REGRESSIONS VARYING THE WAY(I) IS CALCULATED

STANDARD ERROR [N]		**Time to include data**	
		0.5 s	**1 s**
Increasing form	**Linear**	0.373	1.184
	Exponential	0.559	0.555
	Logarithmic	0.524	1.176

WITHOUT INCLUDING *(I)*	
STANDARD ERROR [N]	1.385

A graph to analyze hysteresis was obtained for each case in order to have a second criterium and identify which of the six calculation modes for the moving integral performs better.

Compensation with time elapsed data until 1s for either parameter calculation is less accurate than compensation with time elapsed data until 0.5s.

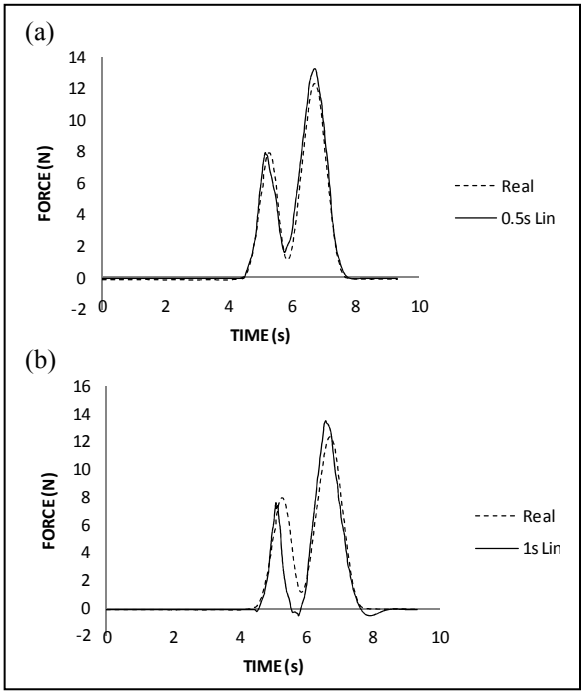

Figure 9. Linear Interpolation.

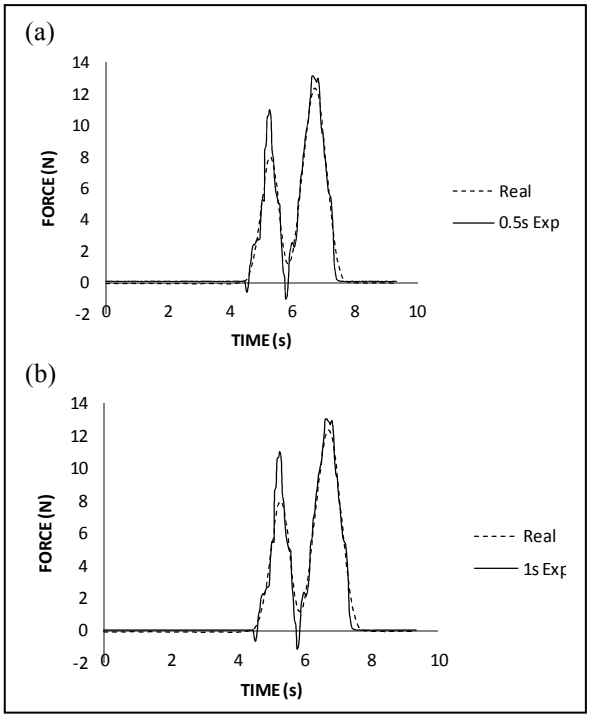

Figure 10. Exponential Interpolation.

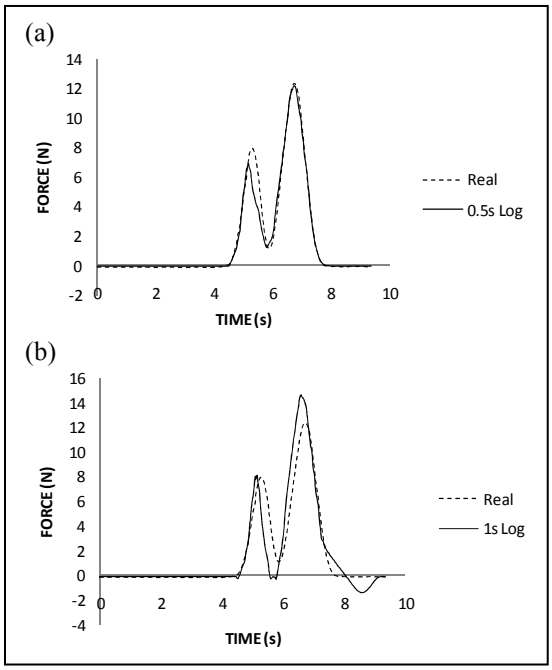

Figure 11. Logarithmic interpolation.

If hysteresis had been completely eliminated with some of the procedures explained previously, only a single line with a 45° slope should appear in the graph, since it'd be the graphic evidence of a one to one relation between the real and the calculated force, regardless the load history.

The graphs in Fig. 12, Fig. 13 and Fig. 14 clearly show an improvement in the hysteresis compensation compared with the results obtained without including the moving integral in the regression (Fig.8(b)) reflected in a significant reduction of the area bounded between the lines.

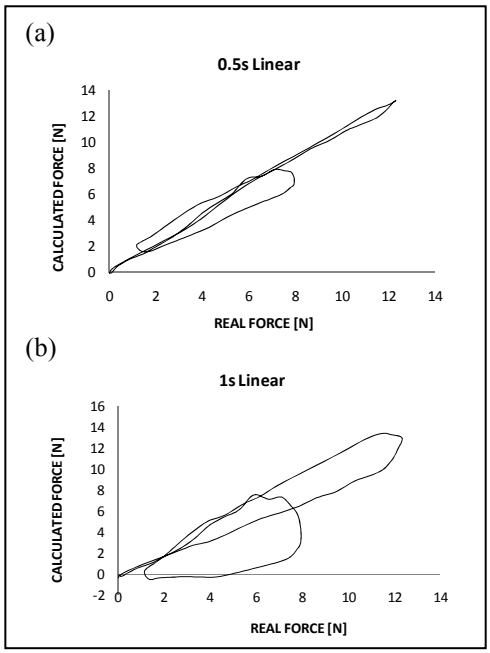

Figure 12. Hysteresis with linear interpolation.

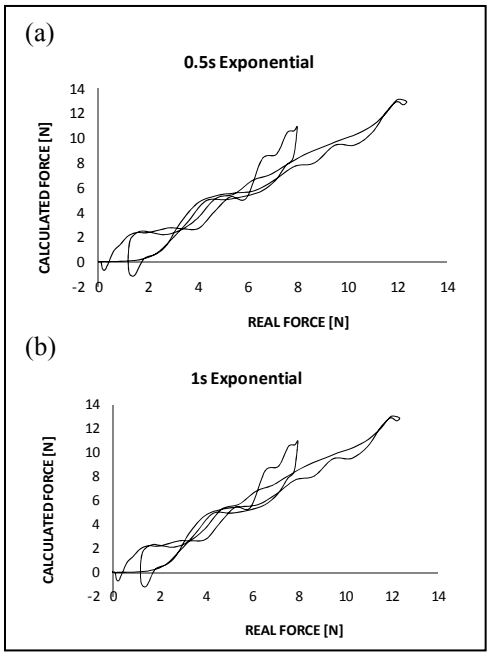

Figure 13. Hysteresis with exponential interpolation.

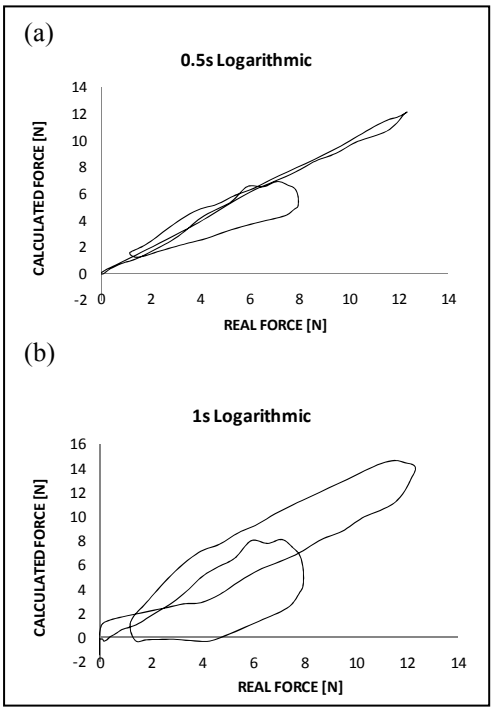

Figure 14. Hysteresis with logarithmic interpolation.

Finally it is graphically evident that the regression made with linear increasing, and 0.5s previous data has the lowest area enclosed and is closer to a single straight line. Thus this setup brings the lowest hysteresis.

C. Characteristic Curves

One last step in the calibration process is to find a direct relation between the force applied to the FSR and its electric resistance (R_{FSR}), since the manufacturer offers a very simplified curve of such relation [1].

This can be mathematically developed, from the current-to-voltage circuit configuration showed in Fig. 1, where it can be inferred a relation between V^+ and V_{OUT} as (3).

$$V^+/(RM+R_{FSR})=V_{OUT}/RM \quad (3)$$

From (3) can be inferred a way to calculate R_{FSR} with V_{OUT} data, and is shown in (4).

$$R_{FSR}= RM*((V^+/V_{OUT})-1) \quad (4)$$

Having $RM=2.2k\Omega$ and V^+=+5VDC, a set of R_{FSR} data can be calculated from a previously acquired set of V_{OUT} data and related with its corresponding force values. In this way, a R_{FSR} vs. Force graph can be elaborated (Fig. 15(a)).

In the same way, and taking advantage of the dome installation, a graph relating the pressure over the sensor and its resistance can be constructed. Since the major reason for the realization of the calibration includes human tactile pressure measurement, the units of pressure used are mmHg, and the interest range is from 0mmHg to 100mmHg. Knowing that the dome's flat area is 126.68mm^2, the pressure values were calculated for each force value, and plotted in Fig. 15(b).

V. Discussion

In the development of this calibration process, several non-desired behaviors had to be considered in order to obtain an acceptable mapping of an applied force curve through the output voltage signal obtained from an electric circuit as the one shown in Fig. 1(a).

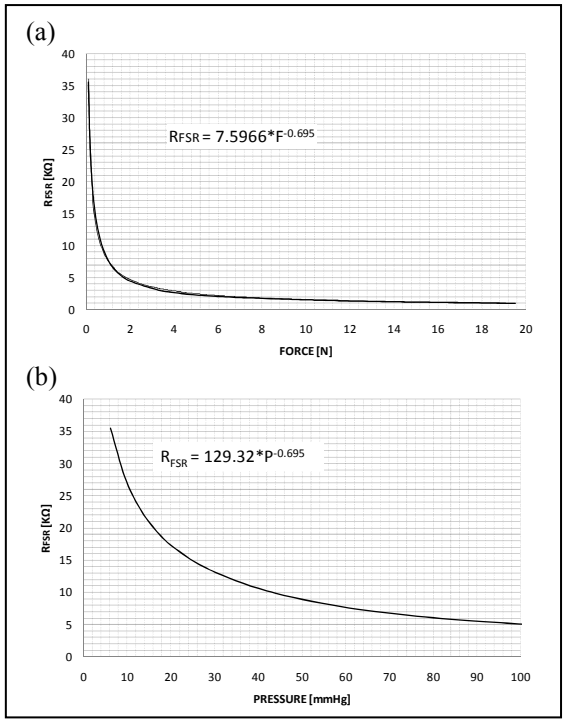

Figure 15. (a) R_{FSR} vs. Force graph and function. (b) R_{FSR} vs. Pressure graph and function.

Creep, although not eliminated, was effectively compensated by processing the acquired data which gives a constant theoretical value of the force.

Something similar happens with the method used for hysteresis compensation. In such way, it is considered that each strategy should preferably be implemented independently since performance may be reduced when both techniques are used simultaneously. Creep compensation should be considered for static measurements, while hysteresis compensation should be performed for dynamic measurements. If both compensations are to be done, special care should be taken for loading speeds below 0.2V/s.

In the same way that has been considered in consulted literature, a calibration process should be done for each sensor to be used, since their physical characteristics and behavior change from one to another. Consequently it becomes necessary to count on with an automatic device that permits reliable repetition of dynamic force appliance and data acquisition. It is vital to acquire enough data to perform a reliable regression process. In this aspect is also relevant to indicate the great importance that the actuating method has on the calibration and measurement process. It has been recognized drastic difference of FSR readings when the actuation or set up conditions are changed.

FSRs show power law behavior within the force range from 0N to 20N (0mmHg to 1200mmHg pressure range) which is congruent with the information given by the manufacturer. When working within in the 0N to 4N range, this is especially important, because is where the most non-linear relation occurs. This implies that for control purposes a linearization procedure is less feasible than in a higher force range, furthermore it denotes the relevance of having an accurate calibration when using these sensors in low pressure / force range products.

Acknowledgment

The authors thank to the director and the staff of the Mechatronics Laboratory of the EAFIT University, for the technical support during the development of this project.

References

[1] Interlink Electronics Inc., "FSR Force Sensing Resistor Integration Guide and Evaluation Parts Catalog," http://www.ladyada.net/media/sensors/fsrguide.pdf , 2002

[2] Sensitronics LLC. "Force Sensig Resistor," Mayo 18 de 2010; http://sensitronics.com/products/force_sensing_resistor.htm

[3] T. R. Jensen, R. G. Radwin, and J. G. Webster, "A Conductive Polymer Sensor for Measuring External Finger Forces," Journal of Biomechanics, vol. 24, no. 9, pp. 7, 1991.

[4] R. S. Hall, G. T. Desmoulin, and T. E. Milner, "A technique for conditioning and calibrating force-sensing resistors for repeatable and reliable measurement of compressive force," Journal of Biomechanics, no. 41, pp. 4, 2008.

[5] National Instruments Corporation. "NI PCI-6013. Low-Cost 200 kS/s, 16-Bit, 16-Analog-Input Multifunction DAQ," May 18, 2010; http://sine.ni.com/nips/cds/view/p/lang/es/nid/11441

[6] P. Wessa. "Free Statistics Software, Office for Research Development and Education, version 1.1.23-r6, http://www.wessa.net